Journal of Materials Chemistry A

Accepted Manuscript

ROYAL SOCIETY OF CHEMISTRY

www.rsc.org/materialsA

Growth of Thermally Stable Crystalline C_{60} Films on Flat-Lying Copper Phthalocyanine

Terry McAfee, Aubrey Apperson, Harald Ade, Daniel B. Dougherty

Department of Physics and Organic and Carbon Electronics Laboratory, North Carolina State University, Raleigh, NC 27695

Keywords: C_{60}, CuPc, Buckminsterfullerene, Copper(II) Phthalocyanine, co-facial

ABSTRACT

We observe thermally stable growth of fcc(111) films of fullerene-C_{60} on top of crystalline, flat-lying, CuPc film structures on graphite using combined grazing incidence wide-angle x-ray scattering and atomic force microscopy. Such a morphology is nearly ideal for bilayer films of C_{60} / CuPc in solar cells. Very similar crystallinity and morphology is observed when varying the film thickness of either material from 5 nm up to more than 100 nm, suggesting that this advantageous solar cell morphology is not only robust, but may actually be preferred compared to the typical mounded fullerene morphology often seen on standing, edge-on aromatic film substrates. The large, ordered domains observed in both materials and the co-facial interface should greatly increase charge carrier mobility leading to increased fill factor. We envision that bilayer films, such as described here, grown on very high quality graphene as a transparent conducting electrode would simultaneously optimize crystallinity and molecular orientation for peak solar cell performance.

I. Introduction

Small molecule organic semiconductors initiated the field of organic photovoltaics[1] (OPVs) and, in the donor-acceptor bilayer device architecture, provided some of the first glimpses of the upward efficiency trends that persist to this day.[2,3] With the advent of new molecules with tunable ionization potentials and good optical absorption properties[4] as well as novel tandem,[5] p-i-n,[6,7] and graded device architectures,[8] progress toward competitive efficiencies is promising.

Most of the advances in small molecule OPVs use molecular beam deposition to, in principle, allow very precise film thickness control down to the single molecular layer. There are advantages to be gained by creating flat donor-acceptor (D-A) interfaces between highly crystalline materials that reduce carrier recombination losses compared to intermixed D-A films.[9,10] The value of this possibility is contingent upon a stable, crystalline, film growth mode. Otherwise, molecular-scale intermixing at the D-A interface occurs, inducing small randomly oriented domains, often without a percolating pathway to the electrodes, which is detrimental to device performance.

Surprisingly, there are relatively few examples of co-facial D-A growth modes in organic donor-acceptor bilayers which are also thermally stable. Often interfacial energies between donor and acceptor layers lead to a strong tendency for dewetting[11] or phase separation.[12-15] Since intermolecular interactions are generally weak in organic molecular materials, it is rare that donor-acceptor interactions are strong enough to stabilize a cofacial growth mode without tipping the balance toward intermixing[16] that would create a non-abrupt (graded) interface. Moreover, kinetic roughening of organic films during growth can lead to a rough donor film which subsequently templates a similarly rough acceptor film.[11]

Interfacial energetics are particularly unfavorable for fullerene acceptor films which have a reasonably strong cohesive energy and relatively weak interaction with substrate molecules. Moreover, nearly isotropic fullerenes tend to have a steric incompatibility with planar aromatic donor molecules and a strong tendency for phase separation even in bulk mixtures.[16] Fullerene films grown on top of flat-lying pentacene consist of crystallites of only tens of nanometers in diameter.[17] A similar morphology is seen for C_{60} films on top of copper phthalocyanine (CuPc) films grown on SiO_2 and the tendency for dewetting

can be greatly accelerated by only modest thermal annealing.[19] In contrast, C_{60} films grown on standing pentacene form large, flat, ordered domains ~ 100 – 1000 nm wide.[18] Similarly, C_{60} films grown on standing diindenoperylene (DIP) exhibit uniformly oriented fcc crystals with the (1 1 1) plane parallel to the substrate[20]. We have argued in the past that controlled dewetting might be of interest for nanometer scale film morphology engineering.[19] However, it is not yet known what particular morphology will be optimal for organic electronic devices and we also need the versatility to create ultra-flat, abrupt, and cofacial donor-acceptor interfaces.

Within a bilayer device geometry (as in bulk heterojunction devices), it is crucial to understand and control relative molecular orientation at donor-acceptor interfaces. This is necessary to allow the most efficient charge transfer across the interface since excited state coupling is strongly orientation dependent. The general intuition is that a co-facial orientation in which π electron clouds are well-coupled promotes charge separation.[21-23] However, one also needs to balance efficient coupling with the possibility of detrimental geminate recombination across the interface.[24,25] This makes the evaluation of orientation controlled bilayers one of the most important problems in organic electronic materials, particularly when the added question of D-A intermixing at the buried interface is considered.[26]

In this paper, we present observations of a thermally stable growth mode of crystalline C_{60} films on top of flat-lying CuPc films on graphite that establish a robust co-facial orientation at the donor-acceptor interface. We take advantage of CuPc films reported previously on graphite,[27] with large crystalline domains the size of which is limited primarily by the substrate defect density. On top of these films, we grow C_{60} that exhibits comparable long-range crystalline ordering and flat surface morphology that is stable to extensive annealing at 150℃. Crystal structure is inferred from GIWAXS and reveals an expected fcc (111) oriented film alongside a coexisting (122) orientation induced by substrate defects. Atomic force microscopy images show that the C_{60} films exhibit flat terraces on top of CuPc domains with steps heights only on the order of a single molecule. This donor-acceptor film structure and morphology enables a stable and abrupt co-facial interface between CuPc and C_{60} and could be used in operational solar cells employing graphene as a transparent electrode. More immediately, this is an

important model experimental system for the ongoing assessment of the nature of co-facial interaction between fullerene acceptors and aromatic donors.[21-23]

II. Experimental Methods

C_{60} (98%) and CuPc (95%) was obtained from Sigma-Aldrich and loaded, as received, into quartz and boron nitride crucibles, respectively. The crucibles were then outgassed for ~24 hours in high vacuum prior to film growth. HOPG was exfoliated using scotch tape immediately before loading into the deposition chamber. C_{60} and CuPc thin films were grown using thermal evaporation at pressure < 2.0 x 10^{-6} torr in a high vacuum chamber with a base pressure of 10^{-9} torr. Deposition rates, monitored using a quartz crystal microbalance, between 0.01Å/s and 0.2Å/s, typically .05Å/s, were used during film growth. AFM was carried out in AC mode in air using a commercial instrument (Asylum Research MFP-3D). Commercial AFM tips (Budget Sensors, Tap300AL-G) had a nominal radius of ~ 10 nm and a nominal resonant frequency of ~ 300 kHz. Annealing was performed in a dry nitrogen glove box with less than 0.1 ppm O_2 and H_2O.

GIWAXS data was acquired at beamline 7.3.3 at the Advanced Light Source[28] at grazing angles between 0.10° and 0.20° above the plane of the substrate. For data acquired on HOPG substrates, the x-rays were incident on a region of the substrate that was visibly flat, uniform, and did not contain flakes. To make the C_{60} scattering peak at Qxy = 0 $Å^{-1}$ and Qz = 0.767 $Å^{-1}$ visible to the reader, particularly for figures 2 a) and c) where the intensity is weak, transformation of the axis to proper q-space, with missing wedge corrections along the q_z axis was not performed for figure 2. Instead, the axis in figure 2 denoted as being approximately q_z and q_{xy}. To allow the reader to access the accuracy of the crystal orientations assigned in this paper, simulated GIWAXS peak locations have been overplotted on the data from figures 2 c)

and d), but with transformation of the axis to proper q-space, with missing wedge corrections along the q_z axis

III. Results

Figure 1 shows a series of AFM images of C_{60} films of different thicknesses grown on CuPc/HOPG. Overall, the C_{60} film morphology resembles that of the CuPc film substrate well along the striped subdomains. The lateral size of a given C_{60} domain is primarily limited by the size of the flat CuPc subdomain on which it forms. CuPc film morphology and roughness is determined by the quality of the graphene or graphite substrate, which was described previously,[27] Although further study of the morphology dependence of neat CuPc films on defects in graphitic substrates is needed to avoid electrical shorts due to the cracks between CuPc domains, subsequently adding C_{60} should not introduce any additional obstacles for OPV devices.

In Figure 2, we report GIWAXS data for the films shown in Figure 1. Distinct spots in the scattering pattern indicate good crystallinity in the fullerene films. Moreover, the pattern is independent of thickness and does not show any trace of the ring-like features characteristic of typical poorly-crystalline fullerene films with a large distribution of orientations with respect to the substrate plane.

Simulation of the diffraction pattern can be achieved by assigning the film as an fcc fullerene film with coexisting (111) and (122) orientations parallel to the substrate plane. Simulated diffraction patterns, excluding forbidden reflections, for the observed crystal orientations for C_{60} and CuPc are shown in Figure 3. A sharp double peak, centered at Qxy ~ 0 $Å^{-1}$ and Qz ~ 0.95 $Å^{-1}$, which streaks vertically, slightly overlapping the [111] reflection of the (111)

orientation, as seen at the very top of figure 2 d), is scattering from the HOPG substrate, . The [111] reflection of the (111) orientation is seen at Qxy = 0 $Å^{-1}$ and Qz = 0.767 $Å^{-1}$. The [111] reflection of the (122) orientation is seen at Qxy = 0.209 $Å^{-1}$ and Qz = 0.738 $Å^{-1}$. We find that the relative intensity ratio of these two reflections is the same for all samples to within our experimental sensitivity, showing that there is no strong thickness dependence to the creation of the coexisting orientations.

The (111) orientation has been previously reported for similar C_{60} films of a fixed thickness on CuPc / HOPG.[23] Our data indicates an unusual (122) orientation also exists which we presume is nucleated at defects. The AFM data in Figure 1 clearly shows two distinct morphological features in the form of large flat domains as well as smaller granular features. Correlation to the GIWAXS data strongly suggests that the flat domains are the (111) orientation, exemplified by the domain in the bottom left of figure 1 (c) and the more granular features are the (122), exemplified by the small rough domains in the bottom right of figure 1 (c), which are evidently less prevalent in terms of area coverage.

Figure 4 demonstrates the crucial new observation of the thermal stability of C_{60} films when grown on flat-lying CuPc. A 30 nm C_{60} / 150 nm CuPc / HOPG film was characterized by AFM both as-grown, shown in figure 4 a), and after annealing at 105˚ C for 48 hrs, with no apparent changes to the topography. The same sample was further annealed at 150˚ C for 24 hrs, and characterized by AFM, shown in figure 4 b), as well as by GIWAXS, shown in figure 4 c), showing no evidence of a surface nor bulk morphology change due to annealing. This is in dramatic contrast to our previous observations of thermal dewetting that results in C_{60} mound coarsening on CuPc/Si substrates.[19]

IV. Discussion

Both AFM and GIWAXS show that the C_{60} film morphology and crystallinity and mosaicity is essentially the same for 5.5, 30, and 150 nm C_{60} / 30 nm CuPc / HOPG, as well as for 30 nm C_{60} / 150 nm CuPc / HOPG. This thickness independence typifies a cofacial growth mode of fullerene –C_{60} on flat

CuPc that is not commonly observed in donor-acceptor bilayers. Most importantly, the film morphology is very stable to thermal annealing, indicating a relatively strong cofacial interaction at the flat donor-acceptor interface compared to other edge-on films.[19] In particular, the fact that the film morphology is very insensitive to annealing means that there is no significant driving force for intermixing at the interface in this system. Given the observation of this unusual organic film growth mode, it is worthwhile to recount the arguments in favor of a single D-A interface geometry for organic solar cells.

At present, world record power conversion efficiencies for organic solar cells are achieved using the blended polymer-fullerene bulk heterojunction approach.[29] The rationale for this film morphology is to control mesoscale donor-acceptor domain sizes to promote efficient exciton dissociation at D-A interfaces. Domains are engineered to match exciton diffusion lengths so that almost all photo excitations can find their way to an interface before recombining.

However, achieving efficient dissociation of excitons is useless if the charges are not able to transport to the electrode. Typically, once a free hole (electron) is in a donor (acceptor) domain it is not energetically favorable to transfer to the other material. Thus, a continuous pathway to the electrodes is needed for both the donor and acceptor materials. It is challenging to ensure such continuous pathways in BHJ devices. Without numerous percolation paths to the electrodes, charges can become trapped, leading to bimolecular recombination. This makes it challenging to simultaneously optimize both exciton dissociation and bimolecular recombination in a BHJ device.

The layered and crystalline features of the C_{60} / CuPc bilayer films we have created represent a possible alternate approach to meeting this challenge. The large, flat, 3D, single crystal island growth in both the CuPc and C_{60} is advantageous for minimizing recombination. The charges from dissociated excitons not only have a continuous path to the electrode in the donor/acceptor material, the shortest path to the electrode is located within a *single-crystal* domain. This means that charge traps and bimolecular recombination will be limited by charge extraction at the electrodes, which can be easily improved with choice of electron/hole blocking layers and choice of metal for the cathode.

For this reason, we consider it still an open question to what extent bilayer devices can be further improved for organic solar cell technology. Charge transport can be efficient and bimolecular recombination suppressed in a bilayer. However, exciton dissociation will be much less efficient than in a BHJ. Our results here and in our previous CuPc/graphene study[27] also indicate the importance of using very high quality substrates for optimizing crystalline order in small molecule OPV materials. Both for fullerene films and the CuPc substrates on which they are grown, preexisting defects on growth substrates can nucleate secondary crystal orientations. The resulting disorder in unfavorable for charge transport and needs to be avoided. Similar recent observations for pentacene film growth on graphene suggest that these ideas are broadly applicable to small molecule films grown on graphitic substrates.[30]

Thus, an organic solar cell technology based on D-A bilayer will look much more like traditional photovoltaic technologies where crystalline materials are important and single "p-n" junctions are used to establish a built-in electric field. In highly crystalline bilayer device, we will still need to use the chemical potential difference at the D-A interface to dissociate excitons. In the current state of the art, we still need to improve carrier mobilities and exciton diffusion lengths in both donor and acceptor materials. However, this device morphology has advantages in terms of recombination losses as already mentioned and also lends itself to efficiency improvements through the tandem cell construction.[5]

The stability of this system under thermal annealing indicates a distinct advantage to OPV device longevity compared to typical fullerene based BHJ films. First, it demonstrates that the co-facial C_{60}:CuPc interface interaction not only induces large, ordered, crystal growth of the C_{60} film, but is also in a preferred, thermally stable, equilibrium. It has been shown[31] that a major source of degradation in C_{60} films is due to UV-induced polymerization of the C_{60}, which has been demonstrated to be reversible when annealed at 110 °C.[14] Our films are compatible with this annealing treatment, unlike typical, quasi-stable,-fullerene BHJ films which undergo morphological changes under annealing at 110 °C.[32]

V. Summary and Conclusions

In summary we report thermally stable, cofacial, growth of fcc fullerene-C_{60} films on flat-lying CuPc films on graphite. This contrasts sharply with the typical granular, polycrystalline C_{60} film

morphology found on edge-on organic film substrates.[17,19] We observe that the C_{60} film morphology remains the same for 5.5, 30, and 150 nm C60 / 30 nm CuPc / HOPG, as well as for 30 nm C60 / 150 nm CuPc / HOPG. There is only minor crystalline disorder in the form of an alternate fcc (122) orientation with respect to the substrate plane, which we believe is related to nucleation at substrate defects. Most importantly, we observe no tendency for fullerene dewetting, even after annealing. This very stable growth mode indicates a strong interaction at the D/A interface. This is consistent with the general intuition in the organic photovoltaic community about the value of co-facial interactions between planar aromatic species and fullerenes to enhance coupling for OPVs.[21-23]

These observations are important for confirming that co-facial interactions between C_{60} and CuPc can be relatively strong and possibly promote efficient charge transfer in OPVs. In addition, the high crystalline quality of both donor and acceptor films points to very efficient charge transport after separation that is likely to minimize bimolecular recombination. If the recent trend of improving small molecule film quality continues, it will be worthwhile to consider whether the simplest bilayer OPV architecture should be re-visited and explored in functioning devices.

VI. Acknowledgements

This work was equally supported by the U. S. Department of Energy (DE-FG02-98ER45737) and NSF CAREER award DMR-1056861 for characterization and growth, respectively. TM was partially supported by GAANN Fellowships.

Figure1.

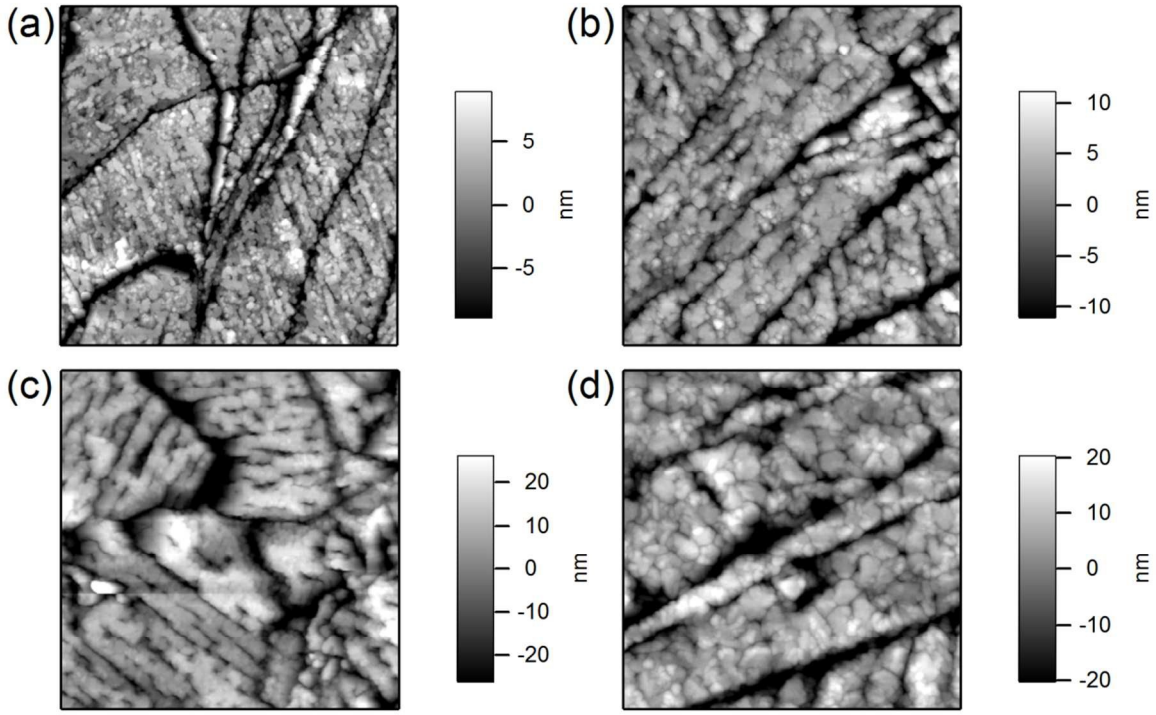

Figure1. Figure caption.

2 um x 2 um AFM on a) 5.5 nm C60 / 25 nm CuPc / HOPG, b) 30 nm C60 / 25 nm CuPc / HOPG, c) 30 nm C60 / 150 nm CuPc / HOPG, d) 150 nm C60 / 25 nm CuPc / HOPG

Figure 2.

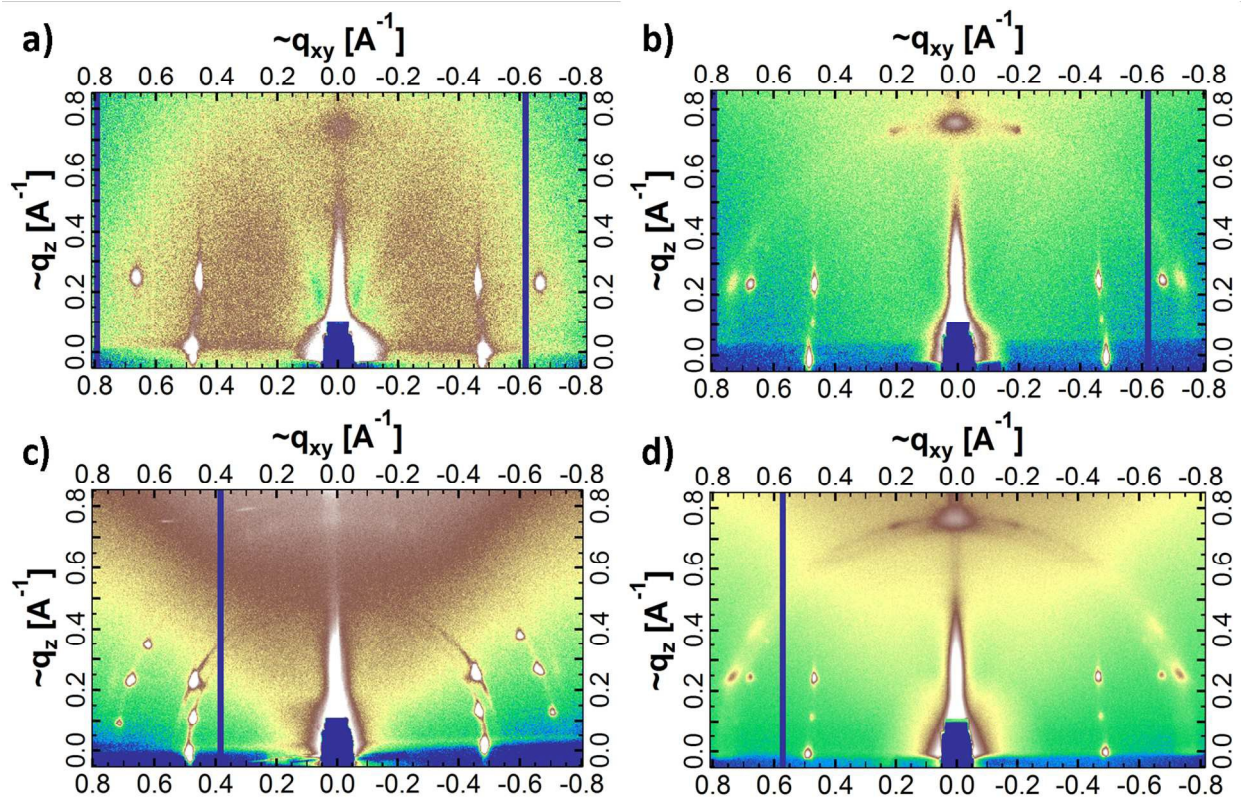

Figure 2 Caption:

GIWAXS acquired at 0.15 Deg incidence angle on a) 5.5 nm C_{60} / 25 nm CuPc / HOPG, b) 30 nm C_{60} / 25 nm CuPc / HOPG, c) 30 nm C_{60} / 150 nm CuPc / HOPG, d) 150 nm C_{60} / 25 nm CuPc / HOPG

Figure 3

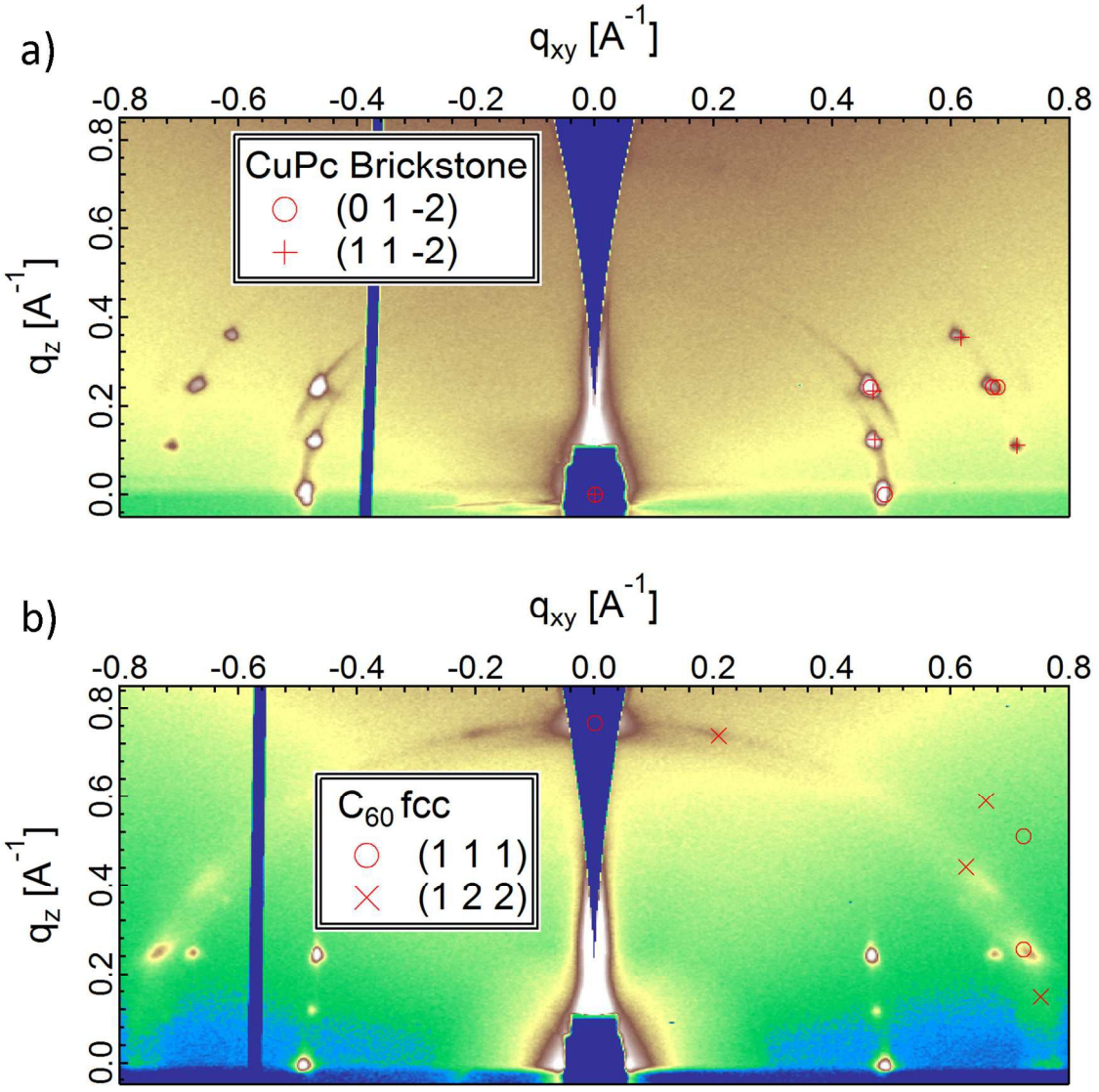

Figure 3 Caption:

Simulated GIWAXS scattering peak locations for CuPc Brickstone (0 1 -2) and (1 1 -2) crystals overplotted on forbidden wedge corrected data from the 30 nm C_{60} / 150 nm CuPc / HOPG film, shown in part a), and C_{60} FCC (1 1 1) and (1 2 2) crystal overplotted on forbidden wedge corrected data from the 150 nm C_{60} / 25 nm CuPc / HOPG film, shown in part b).

Figure 4

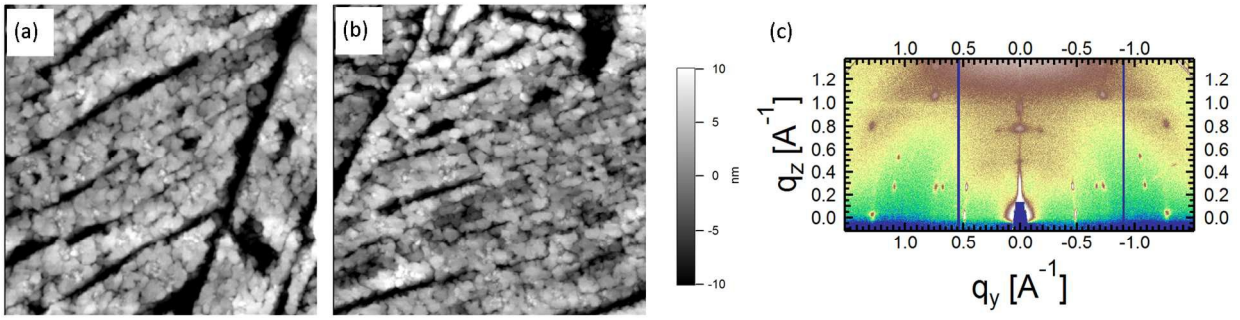

Figure 4 Caption:
2 um x 2 um AFM data on both a) As-Grown and b)post-annealing at 150˚ C for 24 hrs, and c) GIWAXS data (post-annealing at 150˚ C for 24 hrs), all acquired on the same 30 nm C_{60} / 25 nm CuPc / HOPG sample.

VII. References

(1) Tang, C. W. *Applied Physics Letters* **1986**, *48*, 183.

(2) Peumans, P.; Forrest, S. R. *Applied Physics Letters* **2001**, *79*, 126.

(3) Peumans, P.; Yakimov, A.; Forrest, S. R. *Journal of Applied Physics* **2003**, *93*, 3693.

(4) Chen, Y. H.; Lin, L. Y.; Lu, C. W.; Lin, F.; Huang, Z. Y.; Lin, H. W.; Wang, P. H.; Liu, Y. H.; Wong, K. T.; Wen, J. G.; Miller, D. J.; Darling, S. B. *Journal of the American Chemical Society* **2012**, *134*, 13616.

(5) Che, X. Z.; Xiao, X.; Zimmerman, J. D.; Fan, D. J.; Forrest, S. R. *Advanced Energy Materials* **2014**, *4*.

(6) Riede, M.; Mueller, T.; Tress, W.; Schueppel, R.; Leo, K. *Nanotechnology* **2008**, *19*.

(7) Schueppel, R.; Timmreck, R.; Allinger, N.; Mueller, T.; Furno, M.; Uhrich, C.; Leo, K.; Riede, M. *Journal of Applied Physics* **2010**, *107*.

(8) Pandey, R.; Holmes, R. J. *Advanced Materials* **2010**, *22*, 5301.

(9) Sanchez-Diaz, A.; Burtone, L.; Riede, M.; Palomares, E. *Journal of Physical Chemistry C* **2012**, *116*, 16384.

(10) Credgington, D.; Liu, S. W.; Nelson, J.; Durrant, J. R. *Journal of Physical Chemistry C* **2014**, *118*, 22858.

(11) Kowarik, S.; Gerlach, A.; Schreiber, F. *Journal of Physics-Condensed Matter* **2008**, *20*, 184005.

(12) Li, X.; Chen, Y.; Sang, J.; Mi, B. X.; Mu, D. H.; Li, Z. G.; Zhang, H.; Gao, Z. Q.; Huang, W. *Organic Electronics* **2013**, *14*, 250.

(13) Opitz, A.; Wagner, J.; Brutting, W.; Hinderhofer, A.; Schreiber, F. *Physica Status Solidi a-Applications and Materials Science* **2009**, *206*, 2683.

(14) Piersimoni, F.; Degutis, G.; Bertho, S.; Vandewal, K.; Spoltore, D.; Vangerven, T.; Drijkoningen, J.; Van Bael, M. K.; Hardy, A.; D'Haen, J.; Maes, W.; Vanderzande, D.; Nesladek, M.; Manca, J. *Journal of Polymer Science Part B-Polymer Physics* **2013**, *51*, 1209.

(15) Wei, H. X.; Li, J.; Xu, Z. Q.; Cai, Y.; Tang, J. X.; Li, Y. Q. *Applied Physics Letters* **2010**, *97*, 083302.

(16) Hinderhofer, A.; Schreiber, F. *Chemphyschem* **2012**, *13*, 628.

(17) Conrad, B. R.; Tosado, J.; Dutton, G.; Dougherty, D. B.; Jin, W.; Bonnen, T.; Schuldenfrei, A.; Cullen, W. G.; Williams, E. D.; Reutt-Robey, J. E.; Robey, S. W. *Applied Physics Letters* **2009**, *95*, 213302.

(18) Itaka, K.; Yamashiro, M.; Yamaguchi, J.; Haemori, M.; Yaginuma, S.; Matsumoto, Y.; Kondo, M.; Koinuma, H. *Advanced Materials* **2006**, *18*, 1713.

(19) McAfee, T.; Gann, E.; Ade, H.; Dougherty, D. B. *Journal of Physical Chemistry C* **2013**, *117*, 26007.

(20) Hinderhofer, A.; Gerlach, A.; Broch, K.; Hosokai, T.; Yonezawa, K.; Kato, K.; Kera, S.; Ueno, N.; Schreiber, F. *Journal of Physical Chemistry C* **2013**, *117*, 1053.

(21) Rand, B. P.; Cheyns, D.; Vasseur, K.; Giebink, N. C.; Mothy, S.; Yi, Y. P.; Coropceanu, V.; Beljonne, D.; Cornil, J.; Bredas, J. L.; Genoe, J. *Advanced Functional Materials* **2012**, *22*, 2987.

(22) Jailaubekov, A. E.; Willard, A. P.; Tritsch, J. R.; Chan, W. L.; Sai, N.; Gearba, R.; Kaake, L. G.; Williams, K. J.; Leung, K.; Rossky, P. J.; Zhu, X. Y. *Nature Materials* **2013**, *12*, 66.

(23) Ayzner, A. L.; Nordlund, D.; Kim, D. H.; Bao, Z. N.; Toney, M. F. *Journal of Physical Chemistry Letters* **2015**, *6*, 6.

(24) Zimmerman, J. D.; Xiao, X.; Renshaw, C. K.; Wang, S. Y.; Diev, V. V.; Thompson, M. E.; Forrest, S. R. *Nano Letters* **2012**, *12*, 4366.

(25) Zimmerman, J. D.; Lassiter, B. E.; Xiao, X.; Sun, K.; Dolocan, A.; Gearba, R.; Vanden Bout, D. A.; Stevenson, K. J.; Wickramasinghe, P.; Thompson, M. E.; Forrest, S. R. *Acs Nano* **2013**, *7*, 9268.

(26) Fu, Y. T.; Risko, C.; Bredas, J. L. *Advanced Materials* **2013**, *25*, 878.

(27) McAfee, T.; Gann, E.; Guan, T. S.; Stuart, S. C.; Rowe, J.; Dougherty, D. B.; Ade, H. *Crystal Growth & Design* **2014**, *14*, 4394.

(28) Hexemer, A.; Bras, W.; Glossinger, J.; Schaible, E.; Gann, E.; Kirian, R.; MacDowell, A.; Church, M.; Rude, B.; Padmore, H. In *Xiv International Conference on Small-Angle Scattering*; Ungar, G., Ed. 2010; Vol. 247.

(29) Deibel, C.; Dyakonov, V. *Reports on Progress in Physics* **2010**, *73*, 096401.

(30) Zhang, L. S.; Roy, S. S.; Hamers, R. J.; Arnold, M. S.; Andrew, T. L. *Journal of Physical Chemistry C* **2015**, *119*, 45.

(31) Distler, A.; Sauermann, T.; Egelhaaf, H. J.; Rodman, S.; Waller, D.; Cheon, K. S.; Lee, M.; Drolet, N.; Guldi, D. M. *Advanced Energy Materials* **2014**, *4*, 1400171.

(32) Conings, B.; Bertho, S.; Vandewal, K.; Senes, A.; D'Haen, J.; Manca, J.; Janssen, R. A. J. *Applied Physics Letters* **2010**, *96*, 163301.